Examining the Role of Mitochondria in Ca^{2+} Signaling in Native Vascular Smooth Muscle

JOHN G. McCARRON,* MARNIE L. OLSON,* CALUM WILSON,*[†] MAIRI E. SANDISON,* AND SUSAN CHALMERS*

*Strathclyde Institute of Pharmacy and Biomedical Sciences, University of Strathclyde, Glasgow, UK; [†]Department of Biomedical Engineering, University of Strathclyde, Glasgow, UK

Address for correspondence: John G. McCarron, Strathclyde Institute of Pharmacy and Biomedical Sciences, University of Strathclyde, SIPBS Building, 161 Cathedral Street, Glasgow G4 0RE, UK. *E-mail:* john.mccarron@strath.ac.uk

ABSTRACT

Mitochondrial Ca^{2+} uptake contributes important feedback controls to limit the time course of Ca^{2+} signals. Mitochondria regulate cytosolic [Ca^{2+}] over an exceptional breath of concentrations (~200 nM to >10 μM) to provide a wide dynamic range in the control of Ca^{2+} signals. Ca^{2+} uptake is achieved by passing the ion down the electrochemical gradient, across the inner mitochondria membrane, which itself arises from the export of protons. The proton export process is efficient and on average there are less than three protons free within the mitochondrial matrix. To study mitochondrial function, the most common approaches are to alter the proton gradient and to measure the electrochemical gradient. However, drugs which alter the mitochondrial proton gradient may have substantial off target effects that necessitate careful consideration when interpreting their effect on Ca^{2+} signals. Measurement of the mitochondrial electrochemical gradient is most often performed using membrane potential sensitive fluorophores. However, the signals arising from these fluorophores have a complex relationship with the electrochemical gradient and are altered by changes in plasma membrane potential. Care is again needed in interpreting results. This review provides a brief description of some of the methods commonly used to alter and measure mitochondrial contribution to Ca^{2+} signaling in native smooth muscle.

Key words: Smooth muscle, mitochondria, calcium signalling, imaging

Abbreviations used: [Ca^{2+}], cytoplasmic Ca^{2+} concentration; AM, acetoxymethyl; CCCP, carbonyl cyanide m-chlorophenylhydrazone; CCh, carbachol; DiOC6, 3,3-dihexyloxacarbocyanine iodide; FCCP, carbonyl cyanide-4-(trifluoromethoxy)phenylhydrazone; IP$_3$, inositol 1,4,5-trisphosphate; IP$_3$R, inositol 1,4,5-trisphosphate receptor; JC-1, 5,5′,6,6′-tetrachloro-1,1′,3,3′-tetraethylbenzimidazolylcarbocyanine iodide; LetM1, leucine zippered-EF-hand containing transmembrane protein 1; mAChR3, muscarinic type 3 receptor; MCU, mitochondrial uniporter; mNCX, mitochondrial Na$^+$/Ca^{2+} exchanger; PLC, phospholipase C; PTP, permeability transition pore; rhod-2, rhodamine-like fluorophores; RyR, ryanodine receptor; SR, sarcoplasmic reticulum; TMRE, tetramethylrhodamine ethyl ester; TMRM, tetramethylrhodamine methyl ester; $\Delta\Psi_M$, mitochondrial membrane potential.

FINE CONTROL OF Ca^{2+} SIGNALING AND BIOLOGICAL RESPONSES

Changes in the [Ca^{2+}]$_c$ trigger numerous vascular smooth muscle cell activities, which include cell division, growth, metabolism, contraction, and death. To enable the ion to modulate such a diversity of activities, there are a wealth of different types of Ca^{2+} signals (the Ca^{2+} toolkit, [6,45]) with various amplitudes, durations, and frequencies and the signal may be confined to particular parts of the cell. Each of these features (amplitude, frequency, duration, location) may selectively target Ca^{2+} signals to particular physiological responses. A central requirement for the existence of the various temporal and spatial signals are local feedback processes which shape the Ca^{2+} increase or restrict changes in the [Ca^{2+}]$_c$ to small parts of the cell. Mitochondria are of acknowledged significance in the feedback control of Ca^{2+} signaling [15]. The organelle's facility for rapid Ca^{2+} uptake controls the Ca^{2+} signal and the altered signal is transduced to a biological response by mitochondria themselves or by other parts of the cell.

The two main sources of Ca^{2+} are the extracellular fluid and the intracellular stores (the SR). Ca^{2+} enters the cell from the extracellular fluid via channels on the plasma membrane such as the voltage-dependent and store-operated Ca^{2+} channels. The other main Ca^{2+} source is the SR

store from which release proceeds via two receptor-controlled channels—the IP_3R and the RyR [8,44]. Significantly, the sources of Ca^{2+} are not independent; Ca^{2+} influx regulates Ca^{2+} release and Ca^{2+} release regulates Ca^{2+} influx. For example, Ca^{2+} release from the SR may alter plasma membrane ion channel activity to regulate the membrane potential and Ca^{2+} entry, whereas depletion of the SR of Ca^{2+} activates influx via store-operated Ca^{2+} channels [5,47,53,80]. Thus, a change in $[Ca^{2+}]_c$ arising from the activity of channels in the plasma membrane or the SR will itself regulate ion channel activity to provide feedback control of Ca^{2+} signals.

The strategic positioning of channels, receptors, and organelles is important in facilitating the operation of feedback processes. Various channels, receptors, and organelles combine to become functional units and enable Ca^{2+} to act as either a highly localized signal or to evoke more widespread effects through the cell. For example, in sympathetic neurons, while muscarinic and bradykinin receptors each stimulate PLC to produce IP_3, only bradykinin receptors co-immunoprecipitate with, and activate, IP_3R to evoke Ca^{2+} release [19]. The arrangement enables different responses to be evoked depending on whether PLC is activated by muscarinic or bradykinin receptors; muscarinic receptors play a key role in regulating neuronal excitability [10] and bradykinin receptors mediate inflammation and hyperalgesia [20].

Active IP_3R are positioned near the plasma membrane providing another mechanism for agonists, acting via IP_3, to target specific cellular responses by generating Ca^{2+} rises in specific regions of the cell [74]. For example, in cerebral arteries endothelial membrane projections extend through the internal elastic lamina to adjacent smooth muscle membranes. In the projections, local IP_3-mediated Ca^{2+} release events (referred to as "pulsars") activate intermediate conductance, Ca^{2+}-sensitive potassium channels, which co-localize to the same region, to hyperpolarize the endothelial membrane. The resultant membrane potential change is transmitted from the endothelium to the smooth muscle cells by coupling of the membrane via the projections. In this way localized IP_3-mediated Ca^{2+} release in endothelial cells triggers relaxation in smooth muscle cells [40]. RyR are also organized to contribute to feedback activity and may be coupled to channels on the plasma membrane to form functional units. Local Ca^{2+} release events from RyR (Ca^{2+} sparks), may activate either Ca^{2+}-activated K^+ channels or Ca^{2+}-activated Cl^- channels or both to generate spontaneous transient outward (hyperpolarizing) or inward (depolarizing) currents on the plasma membrane [4,63,80,81]. This facility again permits local Ca^{2+} release via RyR to activate or inhibit smooth muscle function. Another structural element to the organization of Ca^{2+} signals lies in the clustering surface receptors in certain regions on the plasma membrane.

The clustering of surface receptors provides areas with increased sensitivity to extracellular stimuli [77] that contribute to feedback control and achieves local specificity in Ca^{2+} signaling.

Regenerative propagation of the Ca^{2+} rise (a "Ca^{2+} wave") occurs by positive feedback control of the Ca^{2+} rise and is another example of interaction among components, in this case to increase the reach of a local Ca^{2+} signal. In smooth muscle, local Ca^{2+} release from the SR may activate neighboring closely positioned ion channels on the SR to propagate the signal from site to site through the cell [9,32,42,46,50] in a way reminiscent of a "fire-beacon" relay network. An interesting feature of waves in smooth muscle is that the Ca^{2+} rise begins at precisely the same small site on each activation despite the cell being stimulated uniformly across the plasma membrane, indicating that is there is a preferred site of wave initiation [60]. That local precision in wave initiation is also explained by receptor complexes, in this case which contain mAChR3 and IP_3R1 that are structurally and functionally coupled (Figure 1) [60]. mAChR3 and IP_3R co-localize to lie within 40–100 nm of each other to generate junctions which facilitate a privileged delivery of IP_3 to particular IP_3R [60]. This arrangement circumvents the diffuse global signaling that is normally associated with IP_3 and the inositide acts as a targeted, highly localized signal. Specific associations between signaling proteins located at the plasma membrane (e.g., mAChR3) and the SR membrane (IP_3R) is one element of feedback control in the Ca^{2+} toolkit enabling receptors to generate differences in the signaling pathways subsequently activated [28,79].

ROLE OF MITOCHONDRIA IN Ca^{2+} SIGNALING

In addition to the feedback arising from the positioning of channels and receptors, intracellular organelles may also regulate Ca^{2+} signals to contribute to the Ca^{2+} toolkit. Mitochondria may take up and sequester a large amount of Ca^{2+} from the cytoplasm and modulate the time course and amplitude of Ca^{2+} signals and shape the resulting message. The mitochondrial capacity to sequester Ca^{2+} is enormous and the buffer power [100,000; 14] is three orders of magnitude greater than that of cytoplasm [~100; 35]. The mitochondrial buffer power arises largely from the quantities of phosphate within the organelle (~5 mM). After uptake, Ca^{2+} is slowly exported from mitochondria via a Na^+-(or H^+-) Ca^{2+} antiporter mechanism [13].

Mitochondria regulate numerous Ca^{2+} signals including those arising from Ca^{2+} release via IP_3R or RyR or voltage-dependent Ca^{2+} entry across the outside membrane. Interestingly, mitochondrial Ca^{2+} uptake may decrease or increase the amplitude of Ca^{2+} signals. In some cells, mitochondrial
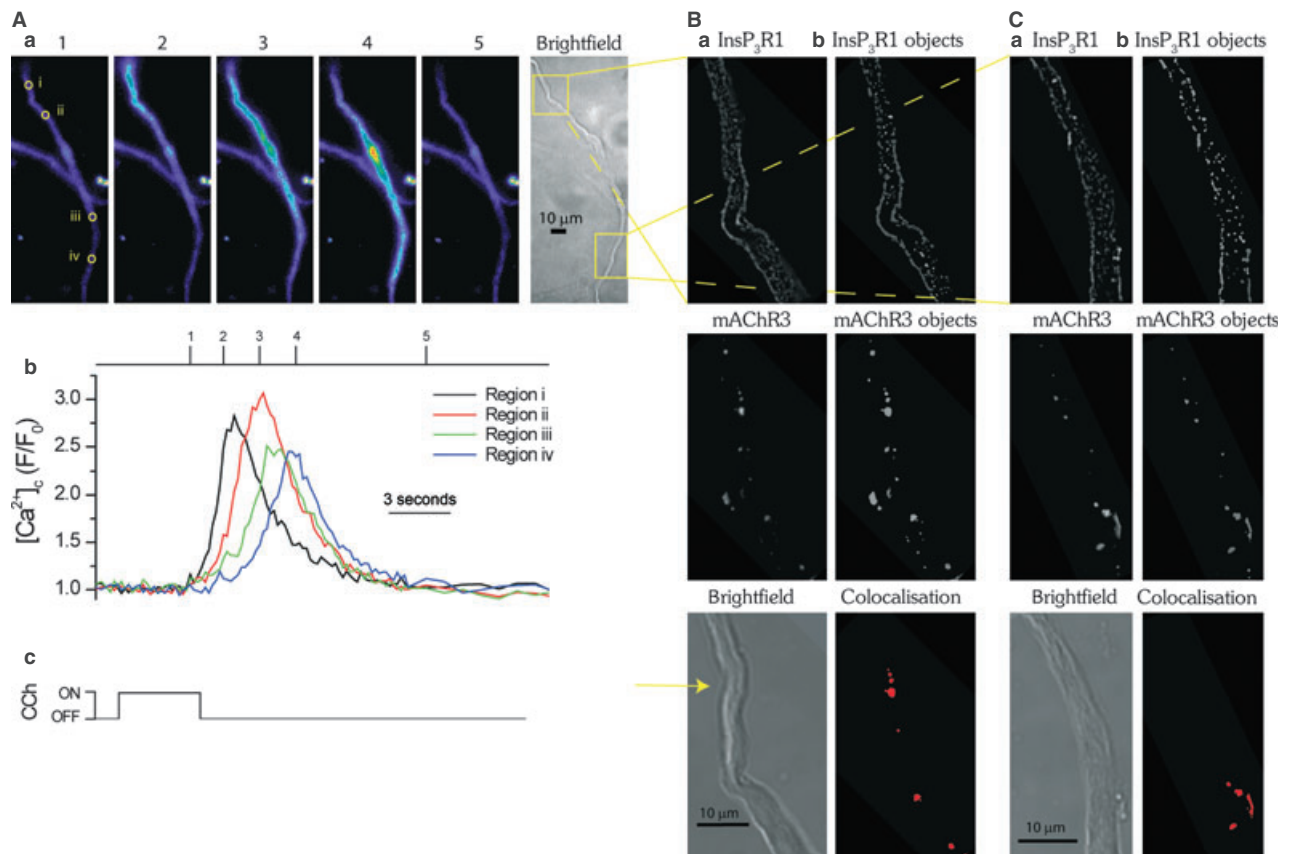
Figure 1. The colocalization of InsP$_3$R1 and mAChR3 at sites of Ca^{2+} wave initiation. Carbachol (CCh, 4 s; **A**c) evoked a Ca^{2+} wave (**A**a, **A**b) which initiated from a single site in a single colonic myocyte (Aa; frame 1, region i) and propagated from there. The Ca^{2+} wave repeatedly initiated from the same site during subsequent carbachol applications (data not shown). The extent of IP$_3$R1 and mAChR3 colocalization was next assessed in the same cell at the site of Ca^{2+} wave initiation and compared to another separate region of the cell (Aa; yellow boxes on bright field image). The cell was fixed, prepared for immunocytochemistry, labeled with IP$_3$R1 monoclonal and mAChR3 polyclonal antibodies, and visualized by confocal microscopy using a fluorescently conjugated secondary antibody (**B**a, **C**a; top and middle panels). Colocalization was quantified using image analysis software ImageJ [65] and the plugin JACoP to examine object-based colocalization. Colocalization of the center of mass of three dimensional IP$_3$R1 and mAChR3 objects created using the 3D object counter plugin (**B**b, **C**b; top and middle panels) were quantified by determining the number of centers from one image that were colocalized with objects from the other image (**B**b, **C**b; bottom panel). In the above experiment, 9.0% of the objects colocalized (9 out of 100 objects detected) at the initiation site and 4.6% colocalized (7 out of 152 objects detected) at the other site. The images shown are from plane 45 of 70 (B; initiation site) and plane 34 of 50 (C; same cell, other site) plane z stacks, each image taken at 150 nm intervals. Brightfield image (Ba, Ca; lower panel) of the same cell; initiation site indicated (Ba; yellow arrow). Note: Scale bar at bottom of bright field images. The images acquired using confocal microscopy (B,C) were rotated for clarity to match the orientation of the images acquired using epifluorescence microscopy (A). From Olson *et al.* [60] with permission.

Ca^{2+} uptake decreases the amplitude of IP$_3$-evoked Ca^{2+} signals; preventing the organelle from taking up Ca^{2+} increases IP$_3$-mediated Ca^{2+} release in cultured hepatocytes and HeLa cells and Ca^{2+} wave velocity in cultured astrocytes [1,7,26]. In other cells (smooth muscle, astrocytes and HeLa cells) mitochondrial Ca^{2+} uptake facilitates IP$_3$-evoked Ca^{2+} release so that preventing mitochondria from taking up Ca^{2+} reduces the amplitude of the Ca^{2+} signal [13,16,23,31,59,73] (see below).

Ca^{2+} signals from RyR activity may also be regulated by mitochondrial Ca^{2+} uptake. Preventing mitochondria from taking up Ca^{2+} prolonged caffeine-evoked [Ca^{2+}]$_c$ increases in aortic and arterial myocytes [25,36]. However, in other

studies, preventing mitochondrial Ca^{2+} uptake did not alter caffeine-evoked SR Ca^{2+} release in cardiac or various smooth muscles [38,72,75,78]. The Ca^{2+} transient arising from voltage-dependent Ca^{2+} entry has an accelerated rate of decline as a consequence of mitochondrial Ca^{2+} uptake and when the uptake is inhibited, the rate of Ca^{2+} decline is substantially slowed (Figure 2) [21,27,49,52].

In controlling Ca^{2+} signals, mitochondria operate over a very wide [Ca^{2+}]$_c$ range (200 nM to >10 μM) [51,64,76]. In the example shown in Figure 2, mitochondria modulate signals over the [Ca^{2+}]$_c$ range 200–600 nM, which demonstrates that mitochondria have a high affinity for Ca^{2+} (in the sub-micromolar range; Figure 2; [see also 64,75]).
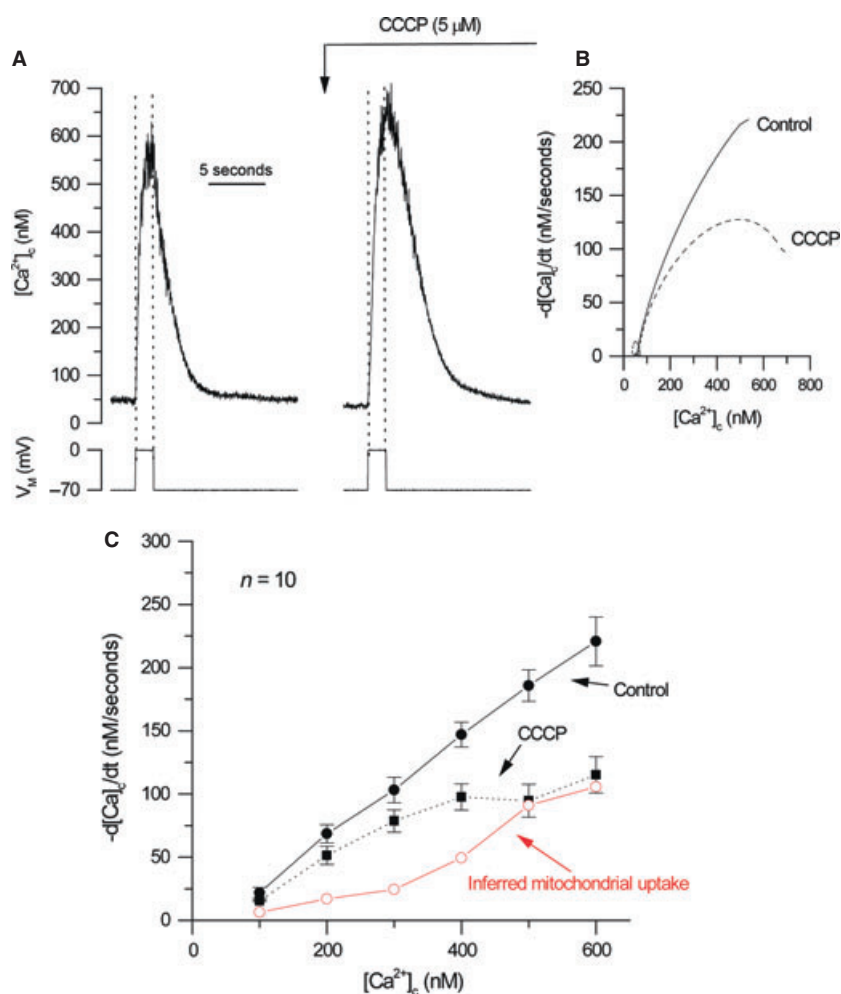
Figure 2. Mitochondria contribute to $[Ca^{2+}]_c$ decline following voltage-dependent Ca^{2+} entry in smooth muscle. (**A**) Depolarization (−70 to 0 mV) activated a voltage-dependent Ca^{2+} current (data not shown) and increased $[Ca^{2+}]_c$ in a single colonic myocyte. CCCP (5 μM) slowed the rate of decline of $[Ca^{2+}]_c$ on repolarization compared with control. (**B**) The rate of decline ($-d[Ca^{2+}]_c/dt$), obtained from high order polynomial fits to the declining phase of the transients, shows a significant slowing when mitochondria were prevented from accumulating Ca^{2+}. (**C**) A summary of the rates of decline for 10 cells in the presence and absence of CCCP. The inferred mitochondrial contribution to the decline of $[Ca^{2+}]_c$ (red line) was obtained by subtracting control rates from those seen in CCCP and shows that mitochondrial Ca^{2+} uptake occurred above 200 nM $[Ca^{2+}]_c$ (from McCarron & Muir [49] with permission).

Interestingly, mitochondria do not appear to alter the rate of rise of the Ca^{2+} transient suggesting that the organelle does not modulate the high local $[Ca^{2+}]$ (>10 μM) near active voltage-dependent Ca^{2+} channels (Figure 2) or the activity of the channels themselves. However, mitochondria do have the capacity to modulate Ca^{2+} signals that are ~2 orders of magnitude larger than the global Ca^{2+} transient from voltage-dependent Ca^{2+} channels and in the tens of micromolar range [67]. One notable example in smooth muscle is mitochondrial regulation of the Ca^{2+} signals which arise from the activity of a single IP_3R cluster ("Ca^{2+} puffs"; Figure 3). When mitochondria are prevented from taking up Ca^{2+} (using uncouplers, complex I inhibitors or uniporter inhibitors), Ca^{2+} puffs are inhibited [59]. This observation suggests the organelle may also have a very low affinity for Ca^{2+} (as Ca^{2+} puffs are >10 μM) and that Ca^{2+} uptake is fast enough to modulate concentrations near ion channels.

The question arises, how do mitochondria, by removing Ca^{2+} from the cytoplasm (i.e., lowering $[Ca^{2+}]$), generate a larger $[Ca^{2+}]_c$ rise? IP_3R is regulated by Ca^{2+}-dependent positive and negative feedback mechanisms. Mitochondrial Ca^{2+} uptake limits a negative feedback inhibition of Ca^{2+} on IP_3R. There are at least two types of Ca^{2+}-dependent negative feedback mechanisms, which may deactivate smooth muscle IP_3R. In the first, a Ca^{2+}-dependent deactivation of IP_3R occurs at $[Ca^{2+}]_c$ which exceed ~300 nM [29]. The onset is rapid and the deactivation persists for ~5 s after the $[Ca^{2+}]_c$ increase ends in permeabilized vascular smooth muscle [30]. Another form of Ca^{2+}-dependent deactivation of IP_3R, once initiated by an increased $[Ca^{2+}]_c$, persisted long (tens of seconds) after $[Ca^{2+}]_c$ had regained resting values, that is became, at least partially, refractory [48,58]. Each of these processes would persistently inhibit Ca^{2+} release via IP_3R. Mitochondrial Ca^{2+} uptake by buffering the Ca^{2+} rise at IP_3R presumably prevents a persistent deactivation of IP_3R to increase the overall release of Ca^{2+} (Figure 4).

The control that mitochondria exert on Ca^{2+} puffs enables the organelle to exert particularly dramatic effects on Ca^{2+} waves and repetitive Ca^{2+} rises (oscillations). When mitochondria are prevented from taking up Ca^{2+}, waves and
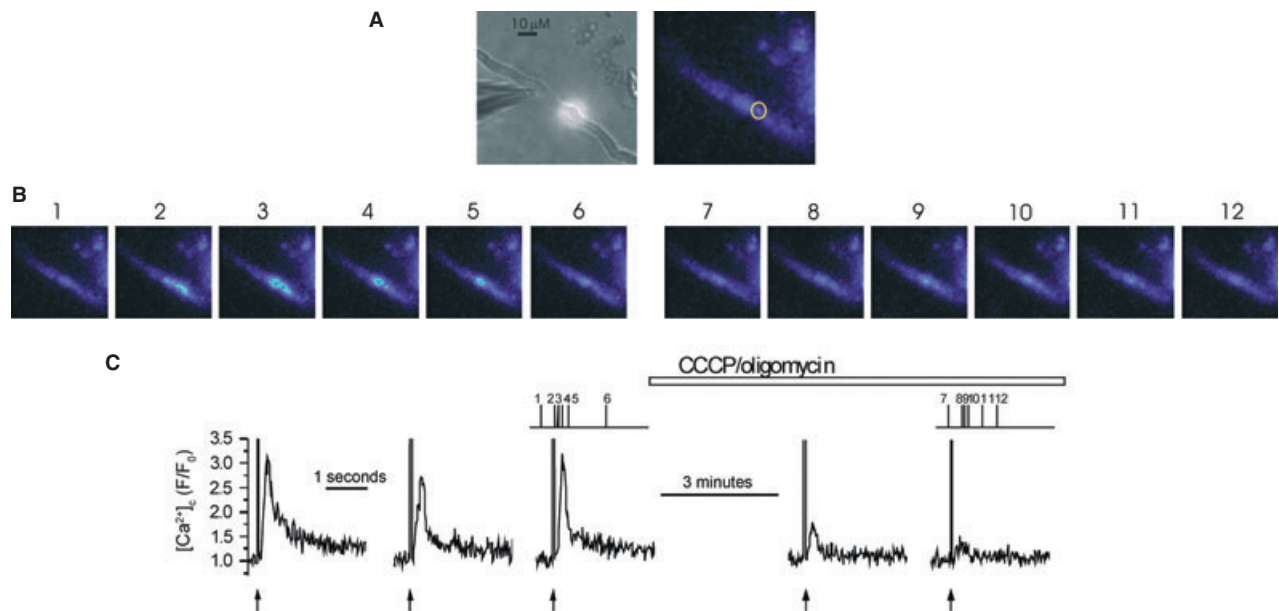
Figure 3. Depolarization of the mitochondrial membrane potential with CCCP inhibits Ca^{2+} release from an IP_3R cluster (Ca^{2+} puffs). At -70 mV, locally photolyzed caged IP_3 (25 μM) ($\uparrow$, **C**) in a ~20 μm diameter region (**A**; bright spot in left hand panel, see also whole cell electrode, left side) evoked Ca^{2+} puffs in a single colonic smooth muscle cell (**B**, **C**). There were two individual Ca^{2+} puff sites activated by photorelease of IP_3. Flash photolysis of IP_3 every ~60 s generated approximately comparable $[Ca^{2+}]_c$ increases (**C**). Superfusion of CCCP (applied with oligomycin; 1 and 6 μM, respectively) while continuing to photolyze IP_3 at ~60 intervals, decreased the amplitude of IP_3-mediated Ca^{2+} puffs (**B**, **C**). The $[Ca^{2+}]_c$ images (**B**) are derived from the time points indicated by the corresponding numbers in (**C**). $[Ca^{2+}]_c$ changes in (**B**) are expressed by color; dark blue low and light blue high $[Ca^{2+}]_c$. Measurements were made from a 3 × 3 pixel box (**A**; right hand panel, white square). The large increase in fluorescence (**C**) at the time of photolysis ($\uparrow$) is artifact from the flash lamp (from Olson *et al.* [59] with permission).

oscillations halt (Figure 5), that is mitochondrial control extends beyond modulation of the time course of a Ca^{2+} rise and the organelle determines whether some signals (waves and oscillations) occur at all.

In some cell types, mitochondria act as a "firewall" and prevent the Ca^{2+} signal from reaching certain regions of the cell. In pancreatic acinar cells, mitochondria are arranged as a "belt" and prevent Ca^{2+} signals from entering the basal part of the cell [62]. However, in smooth muscle, mitochondria do not normally appear to prevent the Ca^{2+} wave from progressing through the cell, but rather the organelle performs a decision-making role to determine whether or not the signal is permitted to progress. If the $\Delta\Psi_M$ is normal and polarized, the Ca^{2+} signal progresses. On the other hand, if $\Delta\Psi_M$ is depolarized (i.e., has a reduced ATP producing capacity) the mitochondria exerts control by inhibiting the local IP_3-mediated Ca^{2+} signal so that the wave does not progress. Thus, as the Ca^{2+} signal regeneratively propagates from site to site through the cell (like a "fire-beacon" network), mitochondria act as "beacon-wardens" and determine whether or not the Ca^{2+} signal is transmitted to the next point of the cell [3,59]. Presumably mitochondria modulate IP_3R, but not voltage-dependent Ca^{2+} channel activity because the organelle is held close to the former, but not to the latter.

MECHANISMS AND DRIVING FORCE FOR MITOCHONDRIAL Ca^{2+} UPTAKE

The large $[Ca^{2+}]$ range over which mitochondria are effective in regulating Ca^{2+} signaling prompted widespread interest into precisely how this is achieved. One mechanism is the MCU, a ruthenium red-sensitive, inwardly rectifying, and highly Ca^{2+} selective voltage-dependent channel of acknowledged importance in Ca^{2+} uptake by the organelle. In voltage-clamp experiments Ca^{2+} flux via MCU did not saturate until $[Ca^{2+}]$ exceeded 100 mM and the $K_{1/2}$ was 19 mM [39]. MCU may fulfill the low affinity role required of the organelle to modulate Ca^{2+} increases near Ca^{2+} channels (e.g., IP_3R). Another proposed Ca^{2+} transporter present on the inner mitochondrial membrane is LetM1 [33]. LetM1, identified in genome-wide siRNA screen studies, is proposed to be a high affinity Ca^{2+}/H^+ exchanger that transports Ca^{2+} into mitochondria during low (<1 μM) global $[Ca^{2+}]_c$ increases when the free mitochondrial matrix $[Ca^{2+}]$ is also low (~5 μM) [33]. LetM1 may fulfill the role required for high affinity Ca^{2+} uptake by mitochondria. However, LetM1 was suggested to be a K^+/H^+ exchanger [56] several years before being proposed as a Ca^{2+} transporter. The Ca^{2+} transport
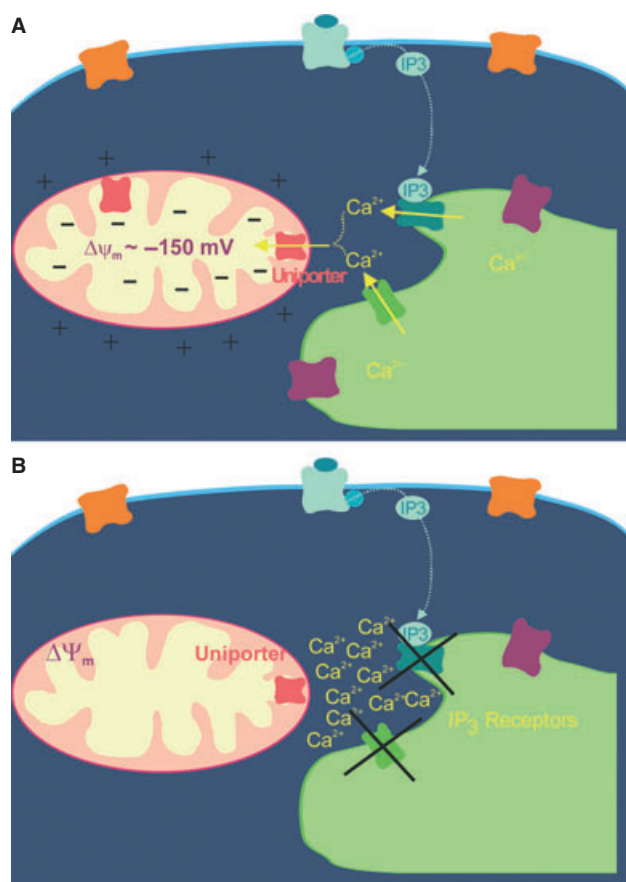
Figure 4. Depolarization of the mitochondrial membrane potential with CCCP inhibits IP$_3$-evoked Ca^{2+} release. (**A**) Mitochondria, by buffering the Ca^{2+} rise at IP$_3$R, prevents a Ca^{2+}-dependent persistent deactivation of IP$_3$R to maintain the overall release of Ca^{2+} from the SR. (**B**) When mitochondria are prevented from taking up Ca^{2+} (using uncouplers, complex I inhibitors or uniporter inhibitors) there is a local increase in [Ca^{2+}] at IP$_3$R promoting Ca^{2+}-dependent negative feedback inhibition of IP$_3$R activity and preventing Ca^{2+} release.

facility attributed to LetM1 is not universally accepted [18,57].

Mitochondrial Ca^{2+} uptake mechanisms pass Ca^{2+} down an electrochemical gradient generated across the inner mitochondrial membrane by an outward movement of H$^+$ via complexes I, III and IV of the electron transport chain. This proton movement establishes both the electrical potential difference ($\Delta\Psi_M$) and the [H$^+$] gradient. The [H$^+$] gradient is significant; cytoplasmic pH is ~7.2 while the pH within the mitochondrial matrix is ~7.8. Indeed the effectiveness of complexes I, III, and IV in exporting H$^+$ is emphasized by considering the average number of free protons within the matrix ($n = CN_A V$; n, number of ions; C, concentration; N_A, Avogadro's number; V, volume). A mitochondrial pH of 7.8 corresponds to a [H$^+$] of ~16 nM (1.58 E^{-8}M). Taking the mitochondrion to be a prolate spheroid with dimensions of 2 μm (major axis) by 0.5 μm

(minor axis) the volume ($V = \frac{4}{3}\Pi a^2 b$ where a is the minor axis radius and b the major axis radius) is 0.26 fL. 1 g-H$^+$/L = 6.023 E^{23} ions/L so that a [H$^+$] concentration of 1.58 E^{-8} M = 9.5 E^{15} ions/L (1.58 E^{-8} × 6.023 E^{23}) and the number of H$^+$ per mitochondrion = 9.5 E^{15} × 0.26 E^{-15} = 2.5. Thus, on average there are only ~2.5 H$^+$ free within the mitochondrial matrix.

Altering Mitochondrial Function and Ca^{2+} Signaling

The low internal proton numbers and significant pH gradient are critical for the performance of mitochondria and mitochondrial control of cell function. Together the transmembrane [H$^+$] gradient and $\Delta\Psi_M$ provide the protomotive force (approximately −180 mV) to drive ADP phosphorylation (catalyzed by the ATP synthase). ATP production approximately doubles with each 10 mV increase in protomotive force [37]. The uptake of Ca^{2+} ions is driven by $\Delta\Psi_M$. Unsurprisingly, a major method of determining the contribution of mitochondria to various cell activities (including Ca^{2+} signaling) is to collapse the proton gradient using drugs such as protonophores and electron transport chain inhibitors. Protonophores (e.g., CCCP and FCCP) are mildly acidic lipophilic compounds that are deprotonated in the mitochondrial matrix to form lipophilic anions. The deprotonated form crosses the inner mitochondrial membrane from the matrix, picks up a proton on the cytoplasmic side, and returns. In this way protonophores collapse the proton gradient and $\Delta\Psi_M$ and, as a result, inhibit ATP synthesis and mitochondrial Ca^{2+} uptake. For example, protonophores slow the rate of [Ca^{2+}]$_c$ decline in smooth muscle (Figure 2) following depolarization-evoked Ca^{2+} entry. This experiment (Figure 2) reveals the ability of mitochondria to accumulate Ca^{2+}, highlights the significance of the proton gradient in mitochondrial Ca^{2+} uptake and demonstrates the ease of use of protonophores to study mitochondrial activity.

However, protonophores may have significant off target effects and care is required in interpreting data from these experiments. Protonophores incorporate into the plasma membrane as well as the inner mitochondrial membrane and by facilitating the flux of protons may substantially alter the cytoplasmic pH. The effect of protonophores may be substantial. Extracellular pH is ~7.4 (i.e., a [H$^+$] of ~40 nM) while cytoplasmic pH is ~7.2 (i.e., a [H$^+$] of ~63 nM). The [H$^+$] is thus highest in cytoplasm and lower in the extracellular space. However, the resting plasma membrane potential (approximately −60 mV; established by K$^+$ permeability) may remain unaltered in the presence of protonophores. Because of its magnitude, the plasma membrane potential will determine the net flux of H$^+$ and the concentration of H$^+$ in the cytoplasm will increase via protonophore activity (i.e., decrease in pH). A 60 mV (inside
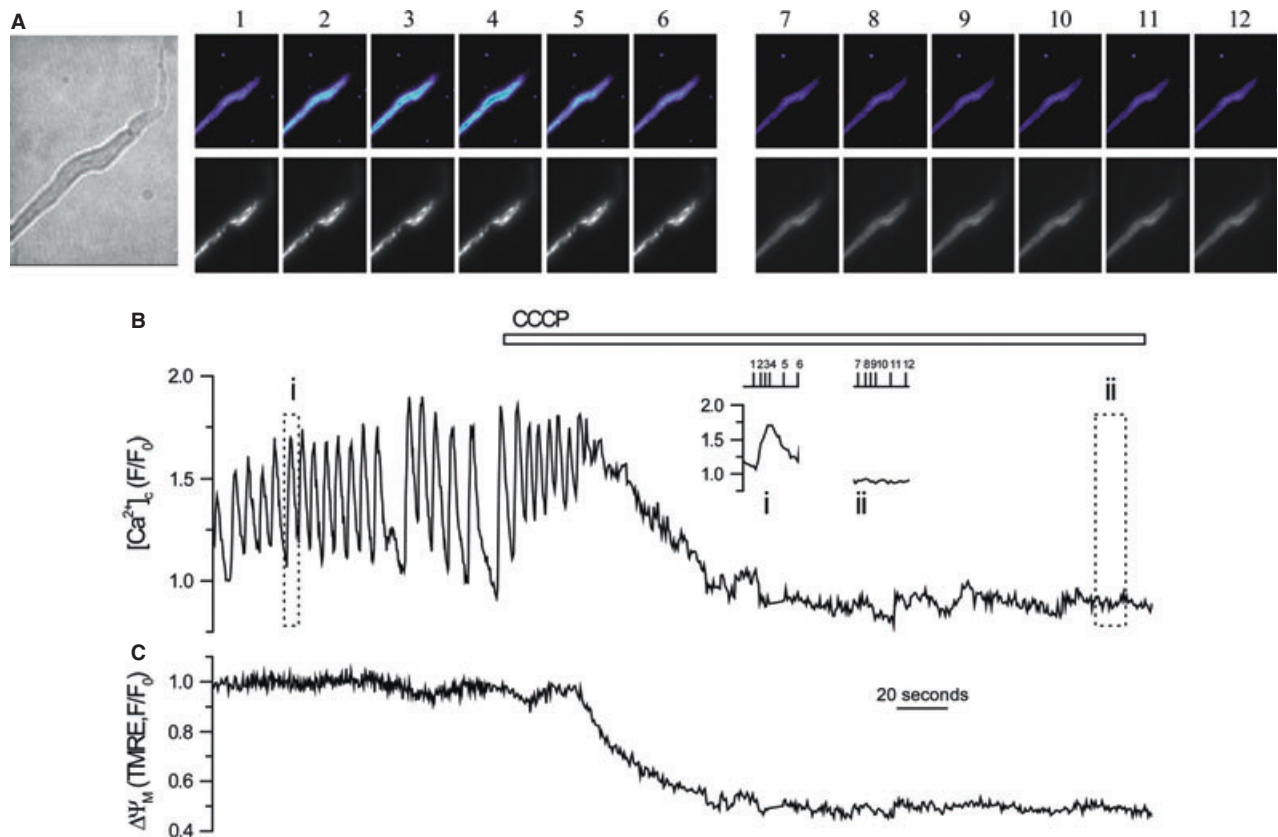
Figure 5. Depolarization of the mitochondrial membrane potential with CCCP blocks Ca^{2+} oscillations. Ca^{2+} oscillations measured with fluo-4 (**A**) upper panel and (**B**) in a single portal vein smooth muscle cell (A left panel) were inhibited by CCCP (applied with oligomycin; 1 and 6 μM, respectively; B open bar). CCCP depolarized $\Delta\Psi_M$ (A lower panel, **C**) as measured by TMRE fluorescence changes and shown as the decrease in fluorescence ratio (C). This suggests that mitochondrial Ca^{2+} uptake is required for Ca^{2+} oscillations to occur (see text). The $[Ca^{2+}]_c$ images (A) are derived from the time points indicated by the corresponding numbers in (B). The insets (B i,ii) are Ca^{2+} responses in boxes i,ii shown on an expanded time base. $[Ca^{2+}]_c$ changes in (A, upper panels) are expressed by color; dark blue low and light blue high $[Ca^{2+}]_c$. $\Delta\Psi_M$ (A, lower panels) is shown as punctate white staining, which decreases with $\Delta\Psi_M$ depolarization. Frames 1–6 (A) are controls (before CCCP/oligomycin) and frame 7–12 after CCCP/oligomycin.

negative) membrane potential difference will result in ~10-fold increase in cytoplasmic $[H^+]$ to 400 nM (i.e., 10 times the external $[H^+]$). Therefore, cytoplasmic pH will decrease from 7.2 to 6.4 when a protonophore is applied. Such a substantial decrease in pH is likely to exert several physiological changes and could result in a false-positive misinterpretation of the effects of protonophores on mitochondrial activity. A way around the pH change is to control cytoplasmic pH (in patch clamp experiments) using high concentrations of H^+ buffers for example, 30 mM HEPES [12,13,49] or to target the protonophore specifically to the mitochondria to ensure significant cytoplasmic pH changes do not occur [11].

Even when changes in pH are considered and controlled, drugs which alter mitochondrial function may also alter the extent of free radical generation or ATP levels in cells (Table 1). Collapse of the proton gradient does not just prevent the production of ATP but results in the ATP

synthase running in reverse to become an ATPase and deplete the cell of ATP, an effect prevented by using oligomycin in combination with drugs that collapse the proton gradient.

When each of these issues is considered and controlled, drugs which alter mitochondrial function provide a powerful experimental tool to examine the role of mitochondria in Ca^{2+} signaling.

Measuring Mitochondrial Function

One of the most common methods of examining mitochondrial function is to optically measure the output of one of several fluorophores that are sensitive to $\Delta\Psi_M$. The most popular belong to various families of compounds, which include rhodamine fluorophores [54], carbocyanins such as JC-1 [66] and DiOC6 [69], merocyanines [34] or oxonols [17]. The major indicators presently used are the rhodamine fluorophores and JC-1 which will be discussed further below.

**Table 1.** Effect of drugs that alter mitochondrial function

Drug	Primary target	Off target/unwanted effects	Other limitations
Uncouplers/protonophores: CCCP, FCCP, DNP, 1799	$\Delta\Psi_M$	Cytosolic pH changes; ATP consumption due to ATPsynthase reversal	Increased H^+ permeability of other cellular membranes
Antimycin A	Complex III blockade (at $Q_{n/i}$ site)		ROS production
Rotenone	Complex I blockade		Can cause ROS production, depending on substrate utilized
Myxothiazol	Complex III blockade (at $Q_{p/o}$ site)		
Ruthenium red	MCU	Ca^{2+} and K^+ channels	Low cell permeability
Ru360	MCU		Low cell permeability
CGP37157	mNCX	>10 μM also inhibits other Ca^{2+} channels	
Oligomycin	ATPsynthase		
Cyclosporin A	Permeability Transition Pore (PTP) by binding cyclophilin D in matrix	Immunosuppresant that also inhibits calcineurin by binding to cytosolic cyclophilins	
Atractyloside/ carboxyactractyloside	Adenine Nucleotide Translocator (ANT) competitive inhibitor, locks ANT into cytosolic-facing conformation & promotes PTP opening		
Bongkrekic acid	Non-competitive inhibitor of ANT, locks ANT into matrix-facing conformation & inhibits PTP opening		
Ionomycin	$Ca^{2+}>Mg^{2+}/2H^+$ exchange	$\Delta\Psi_M$ depolarization when Ca^{2+} is present	
A23187	$Ca^{2+}/2H^+$ exchange	$\Delta\Psi_M$ depolarization when Ca^{2+} is present	Fluorescence that interferes with fluorescent Ca^{2+} dyes (4-bromo-A23187 is non-fluorescent version)
Azide	ATP synthase inhibitor		
Cyanide	Complex IV inhibitor		

Rhodamine fluorophores (e.g., TMRE; TMRM; rhod-123) are fluorescent lipophilic cations that pass readily through lipid bilayers because their charge is dispersed over a large surface area. The mitochondria's negative membrane potential drives the fluorescent lipophilic cations into the matrix [2,68] and fluorophore distribution is described approximately by an Nernstian relationship, that is, ~10-fold accumulation for every 61.5 mV of membrane potential at 37°C. Because of the large mitochondrial surface area to volume ratio, the accumulation of the fluorophore in the organelle changes rapidly (<1 s) with variations in the mitochondrial membrane potential [12]. The more hyperpolarized (increasingly negative) the mitochondria become, the more fluorophore accumulates; the more depolarized (increasingly positive), the less fluorophore accumulates. When these fluorophores are used at low concentrations, changes in fluorescence signal follow changes in dye accumulation in mitochondria. Depolarized mitochondria will have a lower fluorophore concentration and a smaller fluorescence signal. Hyperpolarized mitochondria will have a higher fluorophore concentration and greater fluorescence signal (Figure 6A).

However, these fluorophores are somewhat complicated in their action and at high concentration form non-fluorescent aggregates (i.e., "quench") so that fluorescence emission is reduced. Under these conditions, when mitochondria are hyperpolarized more fluorophore will enter the organelle, but this will cause additional quenching to *decrease* the fluorescent signal. Conversely, when mitochondria are depolarized, fluorophore concentration will decrease and fluorescence emission will now *increase* because the lower fluorophore concentration results in unquenching (Figure 6B). Under continued depolarization, the fluorophore will continue to leave the mitochondria. Eventually, when the fluorophore is unquenched, the fluorescent signal will decline with depolarization (Figure 6B).

Figure 6. Membrane-permeant, lipophilic fluorescent cations can be used to monitor $\Delta\Psi_M$ in "quenched" and "unquenched" modes. These fluorophores equilibrate across membranes in a Nernstian fashion (i.e., ~10-fold per 60 mV). (**A**) at low fluorophore concentration the observed fluorescence is proportional to $\Delta\Psi_M$ (i). A transient $\Delta\Psi_M$ depolarization of an individual mitochondrion in a primary cerebral vascular smooth muscle cell loaded with TMRE (100 nM) resulted in a transient decrease in the fluorescence intensity of the mitochondrial region (ii, black line) with no measureable fluorescence change in the surrounding cytosolic regions (ii, red & green lines) (ii, scale bar = 5 μm), as visualized by epifluorescence microscopy; that is the change in [TMRE] outside the mitochondria, after $\Delta\Psi_M$ depolarization, is presumably rapidly decreased in the larger volume of the cytoplasm so that a change in fluorescence is not measured. (**B**) At higher concentrations these fluorophores aggregate in mitochondria and self-quench, so that the observed fluorescence is no longer directly proportional to $\Delta\Psi_M$. $\Delta\Psi_M$ depolarization relieves this quenching, resulting in a transient *increase* in fluorescence (Bi & Bii). In this case, a transient $\Delta\Psi_M$ depolarization of an individual mitochondrion resulted in a transient increase in the fluorescence intensity of the mitochondrial region (Bii, black line) and an observable dissipation of the released fluorophore into the surrounding cytosolic regions (Bii, colored lines) (ii, scale bar = 5 μm) because of the larger amount of fluorophore being released from mitochondria to the cytoplasm. When the dye is fully unquenched, the fluorescent signal declines as the dye continues to leave the mitochondria.
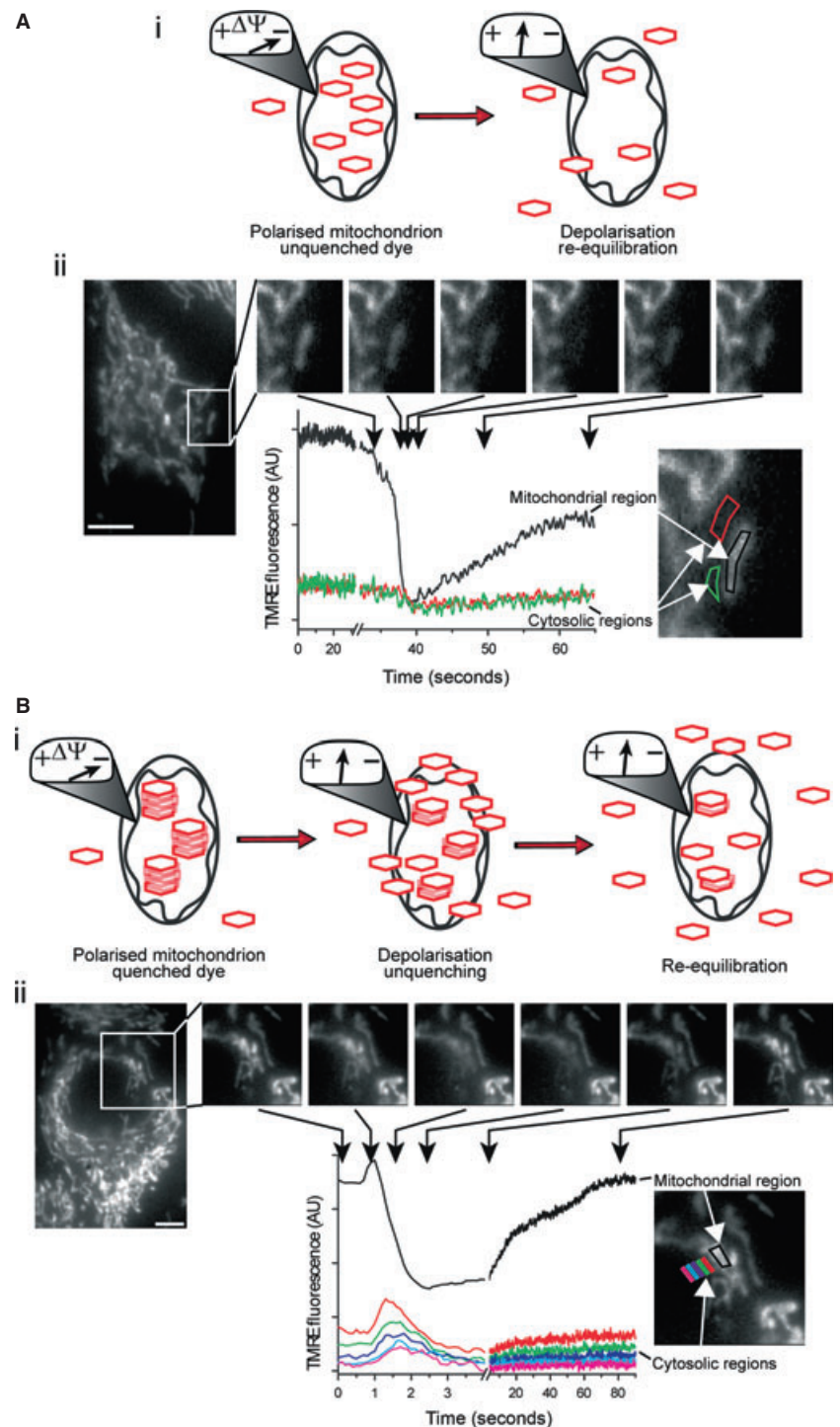
The response from the rhodamine fluorophores therefore depends on the concentration at which they are used, which are referred to as either "quenching" (Figure 6B) or "unquenching" (Figure 6A) modes. The precise concentrations for quenching or unquenching modes should be determined empirically for each cell type. Typically <10 nM will result

produce an unquenched concentration within the mitochondrial while >100 nM will result in quenching. There are advantages to each mode of fluorophore behavior. In unquenching mode, there is considerable sensitivity; changes in $\Delta\Psi_M$ of a few millivolts may be detected and imaging $\Delta\Psi_M$ of single mitochondria is possible. The signal may also be

quantified in unquench mode. The relationship between fluorescence and $\Delta\Psi_M$ is described from the ratio of the free mitochondrial fluorophore concentration to free cytosolic fluorophore concentration and is an exponential function of $\Delta\Psi_M$ [41,61]. However, in practice several difficulties limit quantification. First, the fluorophores may exhibit significant binding to the inner mitochondrial membrane so that most fluorescence comes not from free fluorophore, but from bound fluorophore [61,71]. Changes in binding of the bound fluorophore are non-Nernstian and there is a larger accumulation than is predicted by the Nernst equation alone. While some studies have carefully addressed these issues to quantify $\Delta\Psi_M$ [24,61], the majority of studies measure relative changes in fluorescence as a measure of $\Delta\Psi_M$.

"Quench" mode has the advantage of producing larger signals (when compared with those in unquench mode) which are detected readily at a whole cell (rather than mitochondrial) level resulting in a more straightforward imaging procedure. The response of the fluorophore to membrane potential changes may be highly nonlinear in quench mode, however, and will show both increases and decreases in response to $\Delta\Psi_M$ depolarization. Some consideration must also be given to the sampling frequency; transient changes in whole cell fluorescence in response to $\Delta\Psi_M$ alterations may be missed with low frequency measurements.

As with all agents that are introduced into cells, fluorophores may have some toxicity to mitochondria and cells. Problems can arise from "phototoxicity" when fluorescent molecules react with molecular oxygen to produce free radicals that may damage subcellular components. The lowest possible excitation light intensity should be used. The fluorophores themselves at high concentrations may also inhibit the electron transport chain so the lowest possible fluorophore concentration should be also used.

Rhod-2 have also been used to measure mitochondrial $[Ca^{2+}]$ in native cells [22,23,49]. However, rhod-2 is not straightforward to use and there is the potential for a significant cytosolic contribution to the signal. Rhod-2 AM ester is thought to be a suitable indicator for mitochondrial loading because it is the only cell-permeant Ca^{2+} indicator, which bears a net positive charge. This net positive charge is suggested to promote the uptake of rhod-2 AM into the mitochondrial matrix because of the strongly negative $\Delta\Psi_M$. Once inside the mitochondrial matrix, esterases hydrolyse the AM group leaving the Ca^{2+}-sensitive membrane impermeable form of rhod-2 trapped. However, while rhod-2 bears one net positive charge in the AM form, the de-esterfied rhod-2 bears three net negative charges and (even a partially de-esterified indicator) is unlikely to accumulate in mitochondria. The balance of esterase activity in the cytoplasm and mitochondria will

therefore determine the major source of the signal from rhod-2 and is likely to contribute to variations in results among studies.

The other major class of fluorophore used commonly to measure the mitochondrial membrane potential is represented by JC-1. JC-1 is fluorescent and, like the rhodamine type fluorophores, accumulates in the mitochondria in a membrane potential dependent way. JC-1 has the useful feature of being a ratiometric indicator. In the cytoplasm JC-1 is usually "non-aggregated" (monomeric) and shows green fluorescence emission. When the concentration increases (in mitochondria) JC-1 aggregates and the fluorescence emission shifts from green to red. It is this fluorescence shift that permits ratiometric imaging of $\Delta\Psi_M$. In some studies JC-1 has been used successfully to measure $\Delta\Psi_M$ [43,70], but other investigations have been less successful and report that fluorescence from the aggregated (red) form of the fluorophore may change in a way that is independent of $\Delta\Psi_M$. Moreover, while the monomeric (green) form of JC-1 has been reported to equilibrate on a time scale similar to that of TMRM/TMRE, the *aggregate* (red) form of the dye takes six times longer to equilibrate [43]. The aggregate form is required for JC-1 to act as a ratiometric probe and the differences in time required for equilibration of the two forms of the dye complicate interpretations of fluorescence changes. JC-1 may also report changes in $\Delta\Psi_M$ when none exist, perhaps because of the dye's sensitivity to H_2O_2. Notwithstanding, JC-1 has been used successfully in some studies to image change in $\Delta\Psi_M$.

One additional issue that requires consideration, regardless of the $\Delta\Psi_M$ indicator, is the contribution that the plasma membrane potential makes to the signal measured from mitochondria, that is the fluorescence signal in the mitochondria is not independent of changes in plasma membrane potential. This situation arises because the concentration of fluorophore in mitochondria results from an equilibrium established by the *concentration in the cytoplasm* and the driving force for dye entry to mitochondria provided by $\Delta\Psi_M$. Significantly, the concentration of fluorophore in the cytoplasm is itself an equilibrium involving the *extracellular* dye concentration and the *plasma membrane potential*. The contribution of the plasma membrane potential is significant and there is a 10-fold increase in cytoplasmic dye concentration for a 60 mV inside negative membrane potential. Drugs or physiological activators that change the plasma membrane potential will alter the concentration of fluorophore in the cytoplasm. As a result, there will be a re-equilibration of fluorophore concentration in mitochondria with the new cytoplasmic concentration and a change in mitochondrial fluorescence even in the absence of a $\Delta\Psi_M$ change. This change in fluorescence could result in a misinterpretation of an effect of a drug or activator as altering $\Delta\Psi_M$ when no such change

has occurred. Solutions are either to clamp the plasma membrane potential or to correct the mitochondrial signals after measuring alterations in the plasma membrane potential [12,55,61].

Another significant consideration in the use of these drugs is an absence of spatial control of the organelles affected. One approach to overcome the lack of spatial control has been the development of photoactivatable forms of uncouplers [11]. These photoactivatable uncouplers are membrane permeant, targeted to mitochondria, but are inactive until instructed otherwise by a locally directed pulse of light. Only those mitochondria exposed to the light will be affected by the drug. Individual cells or even single mitochondria can be targeted to generate precise spatial and temporal control. Photoactivateable drugs provide a significant advance in determining mitochondria's subcellular control of Ca^{2+} signals.

PERSPECTIVE

The mitochondrial proton gradient and $\Delta\Psi_M$ drive Ca^{2+} uptake into the organelle. In studying the role of mitochondria in Ca^{2+} signaling, the proton gradient and $\Delta\Psi_M$ are both measured and manipulated experimentally. Measurement of the mitochondrial electrochemical gradient is most often performed using membrane potential sensitive fluorophores. However, the signals arising from these fluorophores have a complex relationship with the mitochondrial electrochemical gradient and are altered by changes in plasma membrane potential. The solution to the latter problem is either to clamp the plasma membrane voltage or to determine the contribution of plasma membrane voltage changes to the mitochondrial signal. In determining the contribution of mitochondria to the cytosolic Ca^{2+} signal a large number of drugs offer a potent mechanism to alter the organelle's ability to take up Ca^{2+}. These drugs alter mitochondrial Ca^{2+} uptake by changing the proton gradient across the inner mitochondrial membrane but may have significant off target effects. The off target effects include cytosolic pH changes, ATP depletion and alterations in free radical production. However, each off target effect may be controlled experimentally so the drugs offer a powerful method to study the role of mitochondria in Ca^{2+} signaling.

ACKNOWLEDGMENTS

REFERENCES

1. Arnaudeau S, Kelley WL, Walsh JV Jr., Demaurex N. Mitochondria recycle Ca^{2+} to the endoplasmic reticulum and prevent the depletion of neighboring endoplasmic reticulum regions. *J Biol Chem* 276: 29430–29439, 2001.

2. Azzone GF, Pietrobon D, Zoratti M. Determination of the proton electrochemical gradient across biological-membranes. *Curr. Top. Bioenerg.* 13: 1–77, 1984.

3. Balemba OB, Bartoo AC, Nelson MT, Mawe GM. Role of mitochondria in spontaneous rhythmic activity and intracellular calcium waves in the guinea pig gallbladder smooth muscle. *Am J Physiol Gastrointest Liver Physiol* 294: G467–G476, 2008.

4. Bao R, Lifshitz LM, Tuft RA, Bellve K, Fogarty KE, ZhuGe R. A close association of RyRs with highly dense clusters of Ca^{2+}-activated Cl^- channels underlies the activation of STICs by Ca^{2+} sparks in mouse airway smooth muscle. *J Gen Physiol* 132: 145–160, 2008.

5. Benham CD, Bolton TB. Spontaneous transient outward currents in single visceral and vascular smooth muscle cells of the rabbit. *J Physiol* 381: 385–406, 1986.

6. Berridge MJ, Lipp P, Bootman MD. The versatility and universality of calcium signalling. *Nat Rev Mol Cell Biol* 1: 11–21, 2000.

7. Boitier E, Rea R, Duchen MR. Mitochondria exert a negative feedback on the propagation of intracellular Ca^{2+} waves in rat cortical astrocytes. *J Cell Biol* 145: 795–808, 1999.

8. Bootman MD, Collins TJ, Peppiatt CM, Prothero LS, MacKenzie L, De Smet P, Travers M, Tovey SC, Seo JT, Berridge MJ, Ciccolini F, Lipp P. Calcium signalling–an overview. *Semin Cell Dev Biol* 12: 3–10, 2001.

9. Bootman M, Niggli E, Berridge M, Lipp P. Imaging the hierarchical Ca^{2+} signalling system in HeLa cells. *J Physiol* 499: 307–314, 1997.

10. Caulfield MP. Muscarinic receptors–characterization, coupling and function. *Pharmacol Ther* 58: 319–379, 1993.

11. Chalmers S, Caldwell ST, Quin C, Prime TA, James AM, Cairns AG, Murphy MP, McCarron JG, Hartley RC. Selective uncoupling of individual mitochondria within a cell using a mitochondria-targeted photoactivated protonophore. *J Am Chem Soc* 134: 758–761, 2012.

12. Chalmers S, McCarron JG. The mitochondrial membrane potential and Ca^{2+} oscillations in smooth muscle. *J Cell Sci* 121: 75–85, 2008.

13. Chalmers S, McCarron JG. Inhibition of mitochondrial calcium uptake rather than efflux impedes calcium release by inositol-1,4,5-trisphosphate-sensitive receptors. *Cell Calcium* 46: 107–113, 2009.

14. Chalmers S, Nicholls DG. The relationship between free and total calcium concentrations in the matrix of liver and brain mitochondria. *J Biol Chem* 278: 19062–19070, 2003.

15. Chalmers S, Olson ML, MacMillan D, Rainbow RD, McCarron JG. Ion channels in smooth muscle: regulation by the sarcoplasmic reticulum and mitochondria. *Cell Calcium* 42: 447–466, 2007.

16. Collins TJ, Lipp P, Berridge MJ, Li W, Bootman MD. Inositol 1,4,5-trisphosphate-induced Ca^{2+} release is inhibited by mitochondrial depolarization. *Biochem J* 347: 593–600, 2000.

17. Cooper CE, Bruce D, Nicholls P. Use of oxonol V as a probe of membrane potential in proteoliposomes containing cytochrome oxidase in the submitochondrial orientation. *Biochemistry* 29: 3859–3865, 1990.

18. Csordas G, Varnai P, Golenar T, Sheu SS, Hajnoczky G. Calcium transport across the inner mitochondrial membrane: molecular mechanisms and pharmacology. *Mol Cell Endocrinol* 353: 109–113, 2012.

19. Delmas P, Wanaverbecq N, Abogadie FC, Mistry M, Brown DA. Signaling microdomains define the specificity of receptor-mediated InsP₃ pathways in neurons. *Neuron* 34: 209–220, 2002.

20. Dray A. Kinins and their receptors in hyperalgesia. *Can J Physiol Pharmacol* 75: 704–712, 1997.

21. Drummond RM, Fay FS. Mitochondria contribute to Ca^{2+} removal in smooth muscle cells. *Pflugers Arch* 431: 473–482, 1996.

22. Drummond RM, Mix TC, Tuft RA, Walsh JV, Jr., Fay FS. Mitochondrial Ca^{2+} homeostasis during Ca^{2+} influx and Ca^{2+} release in gastric myocytes from Bufo marinus. *J Physiol* 522: 375–390, 2000.

23. Drummond RM, Tuft RA. Release of Ca^{2+} from the sarcoplasmic reticulum increases mitochondrial $[Ca^{2+}]$ in rat pulmonary artery smooth muscle cells. *J Physiol* 516 (Pt 1): 139–147, 1999.

24. Gerencser AA, Chinopoulos C, Birket MJ, Jastroch M, Vitelli C, Nicholls DG, Brand MD. Quantitative measurement of mitochondrial membrane potential in cultured cells: calcium-induced de- and hyperpolarization of neuronal mitochondria. *J Physiol* 590: 2845–2871, 2012.

25. Gurney AM, Drummond RM, Fay FS. Calcium signalling in sarcoplasmic reticulum, cytoplasm and mitochondria during activation of rabbit aorta myocytes. *Cell Calcium* 27: 339–351, 2000.

26. Hajnoczky G, Hager R, Thomas AP. Mitochondria suppress local feedback activation of inositol 1,4, 5-trisphosphate receptors by Ca^{2+}. *J Biol Chem* 274: 14157–14162, 1999.

27. Herrington J, Park YB, Babcock DF, Hille B. Dominant role of mitochondria in clearance of large Ca^{2+} loads from rat adrenal chromaffin cells. *Neuron* 16: 219–228, 1996.

28. Hur EM, Park YS, Huh YH, Yoo SH, Woo KC, Choi BH, Kim KT. Junctional membrane inositol 1,4,5-trisphosphate receptor complex coordinates sensitization of the silent EGF-induced Ca^{2+} signaling. *J Cell Biol* 169: 657–667, 2005.

29. Iino M. Biphasic Ca^{2+} dependence of inositol 1,4,5-trisphosphate-induced Ca^{2+} release in smooth muscle cells of the guinea pig taenia caeci. *J Gen Physiol* 95: 1103–1122, 1990.

30. Iino M, Tsukioka M. Feedback control of inositol trisphosphate signalling by calcium. *Mol Cell Endocrinol* 98: 141–146, 1994.

31. Ishii K, Hirose K, Iino M. Ca^{2+} shuttling between endoplasmic reticulum and mitochondria underlying Ca^{2+} oscillations. *EMBO Rep* 7: 390–396, 2006.

32. Jaggar JH, Nelson MT. Differential regulation of Ca^{2+} sparks and Ca^{2+} waves by UTP in rat cerebral artery smooth muscle cells. *Am J Physiol Cell Physiol* 279: C1528–C1539, 2000.

33. Jiang D, Zhao L, Clapham DE. Genome-wide RNAi screen identifies Letm1 as a mitochondrial Ca^{2+}/H^+ antiporter. *Science* 326: 144–147, 2009.

34. Kalenak A, McKenzie RJ, Conover TE. Response of the electrochromic dye, merocyanine 540, to membrane potential in rat liver mitochondria. *J Membr Biol* 123: 23–31, 1991.

35. Kamishima T, McCarron JG. Depolarization-evoked increases in cytosolic calcium concentration in isolated smooth muscle cells of rat portal vein. *J Physiol* 492: 1–74, 1996.

36. Kamishima T, Quayle JM. Mitochondrial Ca^{2+} uptake is important over low $[Ca^{2+}]_i$ range in arterial smooth muscle. *Am J Physiol Heart Circ Physiol* 283: H2431–H2439, 2002.

37. Kawamata H, Starkov AA, Manfredi G, Chinopoulos C. A kinetic assay of mitochondrial ADP-ATP exchange rate in permeabilized cells. *Anal Biochem* 407: 52–57, 2010.

38. Kettlewell S, Cabrero P, Nicklin SA, Dow JA, Davies S, Smith GL. Changes of intra-mitochondrial Ca^{2+} in adult ventricular cardiomyocytes examined using a novel fluorescent Ca^{2+} indicator targeted to mitochondria. *J Mol Cell Cardiol* 46: 891–901, 2009.

39. Kirichok Y, Krapivinsky G, Clapham DE. The mitochondrial calcium uniporter is a highly selective ion channel. *Nature* 427: 360–364, 2004.

40. Ledoux J, Taylor MS, Bonev AD, Hannah RM, Solodushko V, Shui B, Tallini Y, Kotlikoff MI, Nelson MT. Functional architecture of inositol 1,4,5-trisphosphate signaling in restricted spaces of myoendothelial projections. *Proc Natl Acad Sci USA* 105: 9627–9632, 2008.

41. Loew LM, Tuft RA, Carrington W, Fay FS. Imaging in five dimensions: time-dependent membrane potentials in individual mitochondria. *Biophys J* 65: 2396–2407, 1993.

42. Marchant J, Callamaras N, Parker I. Initiation of IP₃-mediated Ca^{2+} waves in Xenopus oocytes. *EMBO J* 18: 5285–5299, 1999.

43. Mathur A, Hong Y, Kemp BK, Barrientos AA, Erusalimsky JD. Evaluation of fluorescent dyes for the detection of mitochondrial membrane potential changes in cultured cardiomyocytes. *Cardiovasc Res* 46: 126–138, 2000.

44. McCarron JG, Bradley KN, MacMillan D, Chalmers S, Muir TC. The sarcoplasmic reticulum, Ca^{2+} trapping, and wave mechanisms in smooth muscle. *News Physiol Sci* 19: 138–147, 2004.

45. McCarron JG, Chalmers S, Bradley KN, Macmillan D, Muir TC. Ca^{2+} microdomains in smooth muscle cell. *Calcium* 40: 461–493, 2006.

46. McCarron JG, Chalmers S, MacMillan D, Olson ML. Agonist-evoked Ca^{2+} wave progression requires Ca^{2+} and IP₃. *J Cell Physiol* 224: 334–344, 2010.

47. McCarron JG, Flynn ER, Bradley KN, Muir TC. Two Ca^{2+} entry pathways mediate InsP₃-sensitive store refilling in guinea-pig colonic smooth muscle. *J Physiol* 525(11): 3–24, 2000.

48. McCarron JG, MacMillan D, Bradley KN, Chalmers S, Muir TC. Origin and mechanisms of Ca^{2+} waves in smooth muscle as revealed by localized photolysis of caged inositol 1,4,5-trisphosphate. *J Biol Chem* 279: 8417–8427, 2004.

49. McCarron JG, Muir TC. Mitochondrial regulation of the cytosolic Ca^{2+} concentration and the InsP₃-sensitive Ca^{2+} store in guinea-pig colonic smooth muscle. *J Physiol* 516: 149–161, 1999.

50. McCarron JG, Olson ML. A single luminally continuous sarcoplasmic reticulum with apparently separate Ca^{2+} stores in smooth muscle. *J Biol Chem* 283: 7206–7218, 2008.

51. McCarron JG, Olson ML, Chalmers S. Mitochondrial regulation of cytosolic Ca^{2+} signals in smooth muscle. *Pflugers Arch* 464: 51–62, 2012.

52. McGeown JG, Drummond RM, McCarron JG, Fay FS. The temporal profile of calcium transients in voltage clamped gastric myocytes from Bufo marinus. *J Physiol* 497 (Pt 2): 321–336, 1996.

53. Ng LC, Gurney AM. Store-operated channels mediate Ca^{2+} influx and contraction in rat pulmonary artery. *Circ Res* 89: 923–929, 2001.

54. Nicholls DG. Simultaneous monitoring of ionophore- and inhibitor-mediated plasma and mitochondrial membrane potential changes in cultured neurons. *J Biol Chem* 281: 14864–14874, 2006.

55. Nicholls DG. Fluorescence measurement of mitochondrial membrane potential changes in cultured cells. *Methods Mol Biol* 810: 119–133, 2012.

56. Nowikovsky K, Froschauer EM, Zsurka G, Samaj J, Reipert S, Kolisek M, Wiesenberger G, Schweyen RJ. The LETM1/YOL027 gene family encodes a factor of the mitochondrial K^+ homeostasis with a potential role in the Wolf-Hirschhorn syndrome. *J Biol Chem* 279: 30307–30315, 2004.

57. Nowikovsky K, Pozzan T, Rizzuto R, Scorrano L, Bernardi P. Perspectives on: SGP

symposium on mitochondrial physiology and medicine: the pathophysiology of LETM1. *J Gen Physiol* 139: 445–454, 2012.

58. Oancea E, Meyer T. Reversible desensitization of inositol trisphosphate-induced calcium release provides a mechanism for repetitive calcium spikes. *J Biol Chem* 271: 17253–17260, 1996.

59. Olson ML, Chalmers S, McCarron JG. Mitochondrial Ca^{2+} uptake increases Ca^{2+} release from inositol 1,4,5-trisphosphate receptor clusters in smooth muscle cells. *J Biol Chem* 285: 2040–2050, 2010.

60. Olson ML, Sandison ME, Chalmers S, McCarron JG. Microdomains of muscarinic acetylcholine and $InsP_3$ receptors create $InsP_3$ junctions and sites of Ca^{2+} wave initiation in smooth muscle. *J Cell Sci* 125 (Pt 22):5315–5328, 2012.

61. O'Reilly CM, Fogarty KE, Drummond RM, Tuft RA, Walsh JV Jr. Quantitative analysis of spontaneous mitochondrial depolarizations. *Biophys J* 85: 3350–3357, 2003.

62. Park MK, Ashby MC, Erdemli G, Petersen OH, Tepikin AV. Perinuclear, perigranular and sub-plasmalemmal mitochondria have distinct functions in the regulation of cellular calcium transport. *EMBO J* 20: 1863–1874, 2001.

63. Perez GJ, Bonev AD, Patlak JB, Nelson MT. Functional coupling of ryanodine receptors to KCa channels in smooth muscle cells from rat cerebral arteries. *J Gen Physiol* 113: 229–238, 1999.

64. Pitter JG, Maechler P, Wollheim CB, Spat A. Mitochondria respond to Ca^{2+} already in the submicromolar range: correlation with redox state. *Cell Calcium* 31: 97–104, 2002.

65. Rasband WS, Image J, U.S. National Institutes of Health, Bethesda, Maryland, USA, http://rsb.info.nih.gov/ij/, 1997–2005.

66. Reers M, Smith TW, Chen LB. J-aggregate formation of a carbocyanine as a quantitative fluorescent indicator of membrane potential. *Biochemistry* 30: 4480–4486, 1991.

67. Rizzuto R, Pinton P, Carrington W, Fay FS, Fogarty KE, Lifshitz LM, Tuft RA, Pozzan T. Close contacts with the endoplasmic reticulum as determinants of mitochondrial Ca^{2+} responses. *Science* 280: 1763–1766, 1998.

68. Ross MF, Da Ros T, Blaikie FH, Prime TA, Porteous CM, Severinall, Skulachev VP, Kjaergaard HG, Smith RA, Murphy MP. Accumulation of lipophilic dications by mitochondria and cells. *Biochem J* 400: 199–208, 2006.

69. Rottenberg H. Membrane potential and surface potential in mitochondria: uptake and binding of lipophilic cations. *J Membr Biol* 81: 127–138, 1984.

70. Salvioli S, Ardizzoni A, Franceschi C, Cossarizza A. JC-1, but not DiOC6(3) or rhodamine 123, is a reliable fluorescent probe to assess delta psi changes in intact cells: implications for studies on mitochondrial functionality during apoptosis. *FEBS Lett* 411: 77–82, 1997.

71. Scaduto RC Jr, Grotyohann LW. Measurement of mitochondrial membrane potential using fluorescent rhodamine derivatives. *Biophys J* 76: 469–477, 1999.

72. Sharma VK, Ramesh V, Franzini-Armstrong C, Sheu SS. Transport of Ca^{2+} from sarcoplasmic reticulum to mitochondria in rat ventricular myocytes. *J Bioenerg Biomembr* 32: 97–104, 2000.

73. Simpson PB, Russell JT. Mitochondria support inositol 1,4,5-trisphosphate-mediated Ca^{2+} waves in cultured oligodendrocytes. *J Biol Chem* 271: 33493–33501, 1996.

74. Smith IF, Wiltgen SM, Parker I. Localization of puff sites adjacent to the plasma membrane: functional and spatial characterization of Ca^{2+} signaling in SH-SY5Y cells utilizing membrane-permeant caged IP_3. *Cell Calcium* 45: 65–76, 2009.

75. Szalai G, Csordas G, Hantash BM, Thomas AP, Hajnoczky G. Calcium signal transmission between ryanodine receptors and mitochondria. *J Biol Chem* 275: 15305–15313, 2000.

76. Szanda G, Koncz P, Varnai P, Spat A. Mitochondrial Ca^{2+} uptake with and without the formation of high-Ca^{2+} microdomains. *Cell Calcium* 40: 527–537, 2006.

77. Thomason PA, Wolanin PM, Stock JB. Signal transduction: receptor clusters as information processing arrays. *Curr Biol* 12: R399–R401, 2002.

78. Vallot O, Combettes L, Lompre AM. Functional coupling between the caffeine/ryanodine-sensitive Ca^{2+} store and mitochondria in rat aortic smooth muscle cells. *Biochem J* 357: 363–371, 2001.

79. Yuan Z, Cai T, Tian J, Ivanov AV, Giovannucci DR, Xie Z. Na^+/K^+-ATPase tethers phospholipase C and IP3 receptor into a calcium-regulatory complex. *Mol Biol Cell* 16: 4034–4045, 2005.

80. Zhuge R, Fogarty KE, Baker SP, McCarron JG, Tuft RA, Lifshitz LM, Walsh JV Jr. Ca^{2+} spark sites in smooth muscle cells are numerous and differ in number of ryanodine receptors, large-conductance K^+ channels, and coupling ratio between them. *Am J Physiol Cell Physiol* 287: C1577–C1588, 2004.

81. Zhuge R, Fogarty KE, Tuft RA, Walsh JV Jr. Spontaneous transient outward currents arise from microdomains where BK channels are exposed to a mean Ca^{2+} concentration on the order of 10 microM during a Ca^{2+} spark. *J Gen Physiol* 120: 15–27, 2002.